

# UC Irvine

## UC Irvine Previously Published Works

### Title

Spatial variations in optical and physiological properties of healthy breast tissue

### Permalink

<https://escholarship.org/uc/item/32w0r8t4>

### Journal

Journal of Biomedical Optics, 9(3)

### ISSN

1083-3668

### Authors

Shah, Natasha

Cerussi, Albert E

Jakubowski, Dorota

et al.

### Publication Date

2004

### DOI

10.1117/1.1695560

### Copyright Information

This work is made available under the terms of a Creative Commons Attribution License, available at <https://creativecommons.org/licenses/by/4.0/>

Peer reviewed

# Spatial variations in optical and physiological properties of healthy breast tissue

**Natasha Shah**

**Albert E. Cerussi**

**Dorota Jakubowski**

University of California, Irvine  
Beckman Laser Institute  
1002 Health Sciences Road  
Irvine, California 92612

**David Hsiang**

**John Butler**

University of California Medical Center  
Department of Oncological Surgery  
101 The City Drive South  
Orange, California 92868

**Bruce J. Tromberg**

University of California, Irvine  
Beckman Laser Institute  
1002 Health Sciences Road  
Irvine, California 92612  
E-mail: tromberg@bli.uci.edu

**Abstract.** Near-infrared (NIR) diffuse optical spectroscopy (DOS) and diffuse optical imaging (DOI) show promise as noninvasive clinical techniques for breast cancer screening and diagnosis. Since NIR methods are based on optical contrast between healthy and diseased tissue, it is essential to characterize the sources of endogenous contrast in normal subjects. We report intra- and inter-subject variation and bilateral asymmetry of the optical and physiological parameters of 31 women using a seven-wavelength NIR frequency-domain photon migration (FDPM) instrument. Wavelength-dependent absorption and reduced scattering parameters ( $\mu_a$  and  $\mu_s'$ , respectively) were measured in four major quadrants and the areolar regions of left and right breasts. These values were used to determine tissue concentrations of oxy-(HbO<sub>2</sub>) and deoxy-(Hb-R) hemoglobin, lipid content, water concentration, and tissue "scatter power." Mean total hemoglobin for premenopausal (PRE) women (20 to 30  $\mu\text{M}$ ) is approximately two-fold higher than for postmenopausal (POST) subjects at all positions. POST women have approximately 50% higher lipid content (50 to 60%) than PRE at all positions. Water concentration on average is 1.8-fold higher for PRE subjects (30 to 40%) than POST. These differences are most pronounced when comparing the areolar complex to the other regions of the breast. In premenopausal women, the areolar regions have 40 to 45% increased total hemoglobin concentration (THC), 20 to 25% lower lipid content, and 30 to 60% higher scatter power versus the quadrants. Small-scale (3 cm) changes in optical properties are negligible compared to large-scale variations over all quadrants, where the intrinsic spatial heterogeneity of healthy breast tissue is 20 to 40% for  $\mu_a$  and 5 to 12% for  $\mu_s'$ . Although no consistent right-left differences are observed in the study population, relative differences between symmetric positions ranged from 18 to 30% for THC, 10 to 40% for adipose, 10 to 25% for water, and 4 to 9% for scattering (674 nm) within an individual. © 2004 Society of Photo-Optical Instrumentation Engineers. [DOI: 10.1117/1.1695560]

Keywords: breast; photon migration; breast optics; near-infrared spectroscopy; non-invasive.

Paper 044018 received Aug. 19, 2003; revised manuscript received Dec. 15, 2003; accepted for publication Dec. 19, 2003.

## 1 Introduction

A variety of near-infrared (NIR) optical methods for the detection, diagnosis, and clinical management of breast cancer are under development. In general, near-infrared (NIR) methods are based on photon migration models and technology, such as diffuse optical spectroscopy (DOS) and diffuse optical imaging (DOI). DOS and DOI methods provide unique quantitative physiological information that can be used in conjunction with conventional medical imaging techniques, such as magnetic resonance imaging<sup>1–3</sup> and ultrasound.<sup>4,5</sup> Recent applications of diffuse optical methods in breast cancer include monitoring chemotherapy,<sup>6</sup> hormonal effects,<sup>7,8</sup> characterizing tumors,<sup>9–11</sup> and assessing disease risk.

In this work, we employ a DOS instrument based on frequency-domain photon migration (FDPM) technology. FDPM utilizes intensity-modulated light to separate and quantify intrinsic tissue absorption and scattering *in vivo*.<sup>12</sup> Measurements of absorption coefficients ( $\mu_a$ ) at multiple wavelengths are used to calculate concentrations of the principal NIR breast tissue chromophores: deoxy-hemoglobin, oxy-hemoglobin, lipids, and water.<sup>13,14</sup> Measurements of the wavelength dependence of the reduced scattering parameter ( $\mu_s'$ ) is related to the size and distribution of biological scatterers.<sup>15,16</sup> Hence, the spectral behavior of both  $\mu_a$  and  $\mu_s'$  can be used for the noninvasive physiological characterization of soft tissues.

Several investigators have demonstrated the ability of DOS and DOI methods to distinguish malignant from benign breast

Address all correspondence to Bruce J. Tromberg, University of California, Irvine, Beckman Laser Institute, 1002 Health Sciences Road, Irvine, California 92612. Tel: 949-824-8367; FAX: 949-824-6969; E-mail: tromberg@bli.uci.edu

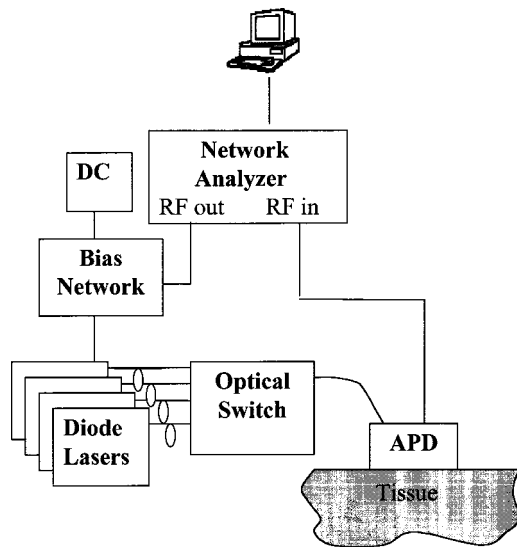


**Fig. 1** Schematic drawing of FDPM instrument and hand-held probe. The main components of the instrument are: network analyzer, DC current source, bias T, diode lasers, optical switch, and avalanche photodiode. See text for detailed description.

lesions *in vivo*.<sup>9–11,17</sup> Preliminary studies have also described the effects of biological factors such as age, menopausal status, hormone use, and menstrual cycle fluctuations on optical properties in normal tissue.<sup>7,18</sup> This study focuses on analyzing the intrinsic spatial variations of breast tissue optical properties in 31 healthy subjects.

Optical property variations across a small subsection of tissue (3 cm) are compared to intrasubject variations over the entire breast. The effects of age and menopausal status on the spatial distribution of optical and physiological parameters are also examined. In addition, since bilateral asymmetry in breasts is common in women, we present data on the typical differences in optical properties between left and right breasts. Our results provide insight concerning the glandular distribution, vascular patterns, and asymmetry within healthy breast tissue. These factors play an important role in characterizing normal breast tissue physiology and understanding the appearance of disease.

## 2 Materials and Methods

### 2.1 Clinical FDPM Measurements

A 1-GHz portable, multiwavelength, high-bandwidth frequency-domain photon migration instrument has been designed and optimized for clinical optical property studies (Fig. 1). The FDPM instrument and theory has been described in detail elsewhere.<sup>19</sup> Briefly, the network analyzer is used to produce modulation frequencies from 50 MHz to 1 GHz. A DC current source is mixed with RF power provided by the network analyzer in a bias network, which distributes power to one of seven laser diodes (674, 780, 803, 849, 894, 915, and 980 nm) to produce amplitude-modulated light. An optical switch delivers light serially from each diode to a 100- $\mu$ m graded index optical fiber that delivers diode laser output to the tissue. A hand-held probe has been designed to house an avalanche photodiode (APD) that records the diffuse light sig-

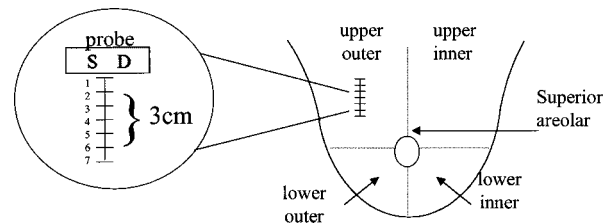


**Fig. 2** Measurement map of healthy volunteers. Each breast is divided into four quadrants: upper outer (UO), upper inner (UI), lower outer (LO), and lower inner (LI). FDPM measurements are made in each quadrant and the superior areolar border (UA). Inset: Location of measurements for small-scale investigation of tissue for five subjects. A series of seven measurements over a 3-cm line were made in 5-mm increments as shown. The probe is aligned so that the source (S) and detector (D) are perpendicular to the scan line.

nals after propagation through the tissue. The probe contains a plastic attachment on the casing to secure the source fiber at a fixed distance of 21 mm from the APD. The network analyzer measures the phase and amplitude of the electronic signal.

Amplitude-modulated light traverses through tissue as a photon density wave (PDW) with a distinct phase and amplitude.<sup>20</sup> The phase shift and amplitude of the PDW after propagation through tissue was determined at each wavelength between 50 to 700 MHz at 1.375 MHz intervals. The range of modulation frequencies was swept repetitively so that each amplitude and phase value represents an average of four measurements. The measurement time over all seven wavelengths is less than a minute. The optical power launched into the subject ranged from 5 to 25 mW for each diode. The instrument response was calibrated before each measurement session on a tissue phantom of known optical properties.

FDPM data was collected from a total of 31 volunteers: 18 premenopausal volunteers ages 18 to 48 years of age (PRE) and 13 postmenopausal women ages 52 to 64 (POST), six of whom were using hormone replacement therapy. Measurements on 28 of the subjects were performed at five distinct positions on each breast (Fig. 2): one position at each of the four quadrants midway between the nipple and the edge of the breast and the superior areolar border. The measurement locations were abbreviated as follows: R=right, L=left, U=upper, L=lower, O=outer, I=inner, and A=areolar, thus LUO denotes the left upper outer quadrant. Three repeat measurements were made by removing and replacing the probe in each location to ensure accuracy. Data from five normal premenopausal volunteers ages 27 to 47 were obtained to provide information on variations in a small region of tissue. A series of seven measurements were acquired in 5-mm increments over a 3-cm line in the upper outer quadrants of both breasts (Fig. 2, inset). Two repeat scans were performed. To ensure reproducible and accurate probe placement, all sites were measured and marked with a surgical pen. All data was collected with subjects resting in the supine position. Experiments were conducted in adherence to University of California (UC) Irvine IRB approved protocols 95-563 and 99-2183. After providing informed consent, volunteers filled out a brief questionnaire, which surveyed pertinent medical history.

**Table 1** Variation of optical and physiological properties in a small volume of tissue for five subjects. Values represent the normalized standard deviation of seven measurements made over a 3-cm span of tissue in the right upper outer quadrant.

Optical/physiological parameter	Normalized standard deviation (%)				
	Subject 1	Subject 2	Subject 3	Subject 4	Subject 5
Age	27	35	35	40	47
$\mu_s'$	3	3	3	6	4
Scatter power	9	16	9	15	2
$S_tO_2$	1	1	1	1	1
THC	9	16	9	14	2
Water	14	12	9	3	12
Lipid	3	5	5	5	4

### 2.2 Theoretical Model

The  $P_1$  approximation to the Boltzmann transport equation was used to extract tissue absorption ( $\mu_a$ ) and reduced scattering ( $\mu_s'$ ) coefficients from frequency-dependent phase and amplitude curves.<sup>21,22</sup> The model employs an extrapolated boundary condition for a semi-infinite geometry.<sup>23</sup> To determine the optical properties from a given set of frequency-dependent data, a Marquardt-Levenburg  $\chi^2$  minimization algorithm was used to simultaneously fit the amplitude and phase by minimizing the difference between the measured values and those predicted by the  $P_1$  approximation.

Physiological properties were calculated from the determined  $\mu_a$  values measured at seven wavelengths by assuming breast tissue is composed of four principal NIR absorbers: deoxy-hemoglobin (Hb-R), oxy-hemoglobin (HbO<sub>2</sub>), lipids, and water. Melanin was not included as an absorber, since the contribution of the epidermis to the total sampled volume of tissue is small.

Hemoglobin concentrations are measured in  $\mu\text{M}$ , lipid content is measured as a mass density percentage, and water is calculated relative to pure water, 55.6 M. Total hemoglobin concentration (THC) is  $[\text{Hb}] + [\text{HbO}_2]$ , and tissue hemoglobin oxygen saturation ( $S_tO_2$ ) is  $([\text{HbO}_2]/\text{THC}) * 100\%$ . The four chromophore concentrations are determined using a least-squares solution to  $E\vec{c} = \mu_a$ , where  $E$  is a  $7 \times 4$  matrix of the molar extinction coefficients and  $\vec{c}$  is the concentration of the chromophores.<sup>24-26</sup> In matrix representation, the chromophore concentration is given by:  $\vec{c} = (\vec{E}^T \vec{E})^{-1} \vec{E}^T \mu_a$ , where  $\vec{E}^T$  and  $\vec{E}^{-1}$  denote the transpose and inverse of the matrix  $\vec{E}$ , respectively.

The spatial heterogeneity in an individual was calculated from the normalized standard deviation (NSD) of the values determined at ten breast measurement locations (five positions on each breast). The NSD equals the standard deviation reflected as a percentage of the mean:  $(\sigma/\bar{x}) * 100\%$ .

### 3 Results

To measure the variability in physiological and optical properties within a small subsection of tissue (3 cm), a series of seven measurements were made in 5-mm increments in the upper outer quadrants of five normal premenopausal subjects. The variability of each parameter was assessed using the normalized standard deviation. The results of the right breast are displayed in Table 1. The change over a 3-cm span is small for  $\mu_s'$  (less than 10%),  $S_tO_2$  (less than 5%), and lipid content (less than 11%). Scatter power and water content are the most variable parameters (10 to 20%). Hemoglobin variability (oxy-, deoxy-, and total) for the five subjects ranges from 2 to 16%.

The spatial variations of healthy breast tissue over the entire breast and age-dependent trends in tissue heterogeneity are displayed in Figs. 3–6. Figure 3 illustrates the mean total

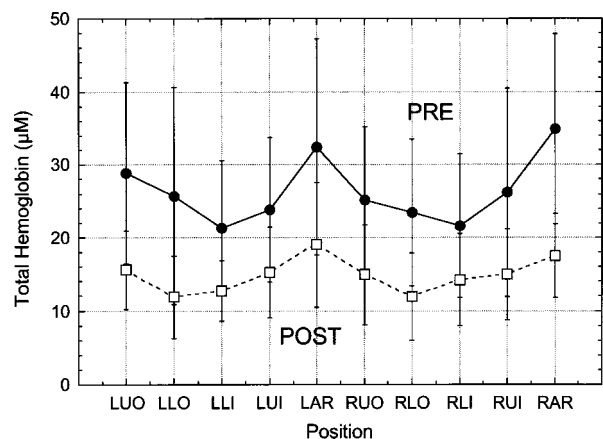


**Fig. 3** Mean total hemoglobin concentration at each measurement position for PRE ( $n=15$ ) and POST ( $n=13$ ) subject groups. Values are determined from wavelength-dependent absorption values for seven wavelengths ranging from 674 to 980 nm. Error bars represent the standard deviation of the mean.

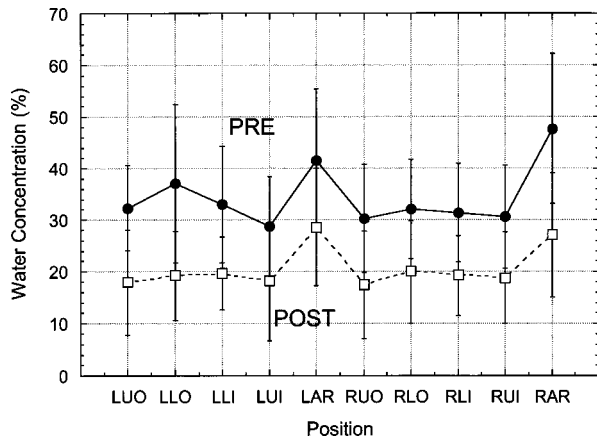


**Fig. 4** Mean water concentration relative to pure water (%) at each measurement site for PRE and POST subject groups. Error bars represent the standard deviation to the mean.

hemoglobin concentration for PRE and POST subject groups at each quadrant position. Mean total hemoglobin for PRE women is approximately two-fold higher than for POST women at all positions. Areolar total hemoglobin levels are approximately 30 to 45% higher than average quadrant levels for PRE subjects, and 25 to 40% higher for POST subjects (89 and 94% confidence interval for left and right breast, respectively). The lower quadrants of PRE women have lower total hemoglobin concentrations relative to the upper quadrants (83% confidence interval).

Water concentration on average is 1.8-fold higher for PRE subjects than POST (Fig. 4). Areolar water concentration is 30 to 50% higher than water concentration for the quadrants for PRE and POST women (84 and 94% confidence interval for left and right breasts, respectively). For PRE women, however, the lower quadrants have more water than the upper quadrants (86% confidence interval); the same pattern is not evident for POST women.

Average lipid content for PRE and POST subject groups at each measurement position are shown in Fig. 5. POST women have approximately 50% higher lipid content than PRE

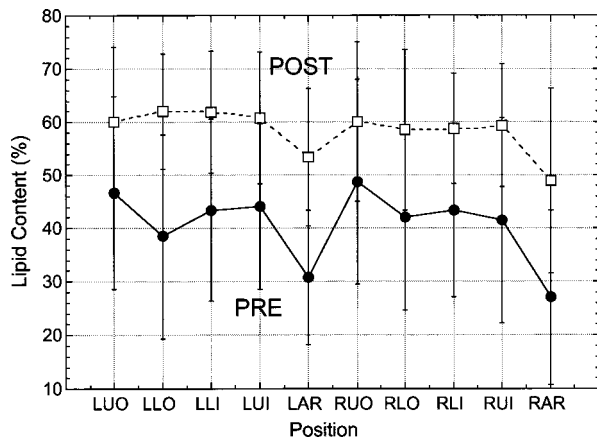
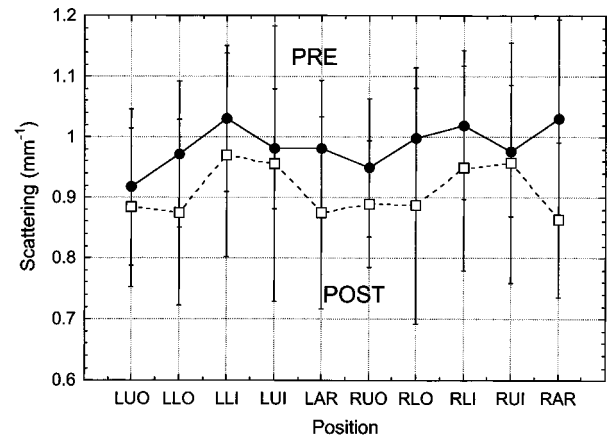
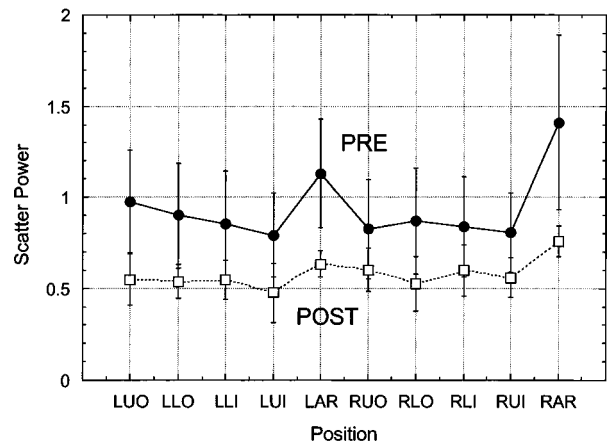


**Fig. 5** Mean lipid content relative to pure lipid (%) at each measurement position for PRE and POST subject groups. Error bars represent the standard deviation of the mean.



(a)



(b)

**Fig. 6** (a) Mean reduced scattering coefficient  $\mu_s'$  at 674 nm at each measurement site for PRE and POST subject groups. Values are calculated from best diffusion model fits to phase and amplitude data. (b) The scatter power ( $\mu_s' = A\lambda^{\text{scatter power}}$ ) versus position for PRE and POST subject groups, where  $A$  is constant  $\mu_s'$  is the reduced scattering coefficient, and  $\lambda$  is the wavelength in nanometers. Error bars represent the standard deviation of the mean.

women at all positions. Areolar lipid content is 25 to 35% lower than average lipid content in the four quadrants for PRE and 10% lower in POST women (74% confidence interval). The lower outer quadrants have lower adipose content than the other three quadrants in PRE women (88% confidence interval); this pattern does not persist in POST women.

The mean  $S_tO_2$  values calculated over the entire breast are  $74 \pm 6$  and  $75 \pm 8\%$  for PRE and POST subject groups, respectively. The left upper outer quadrant exhibits differences between subject groups ( $75.6 \pm 6\%$  for PRE and  $80 \pm 9\%$  for POST), consistent with our previous reports,<sup>7,8</sup> though this trend does not appear in the other measurement positions. Areolar regions have significantly lower saturation values, ( $69.7 \pm 7\%$  for PRE and  $69.8 \pm 12\%$  for POST, 97% confidence interval). There are no significant variations in the quadrants.

A plot of the reduced scattering coefficient at 674 nm for the two subject groups demonstrates that  $\mu_s'$  shows little positional variation [Fig. 6(a)]. The inner quadrants have higher



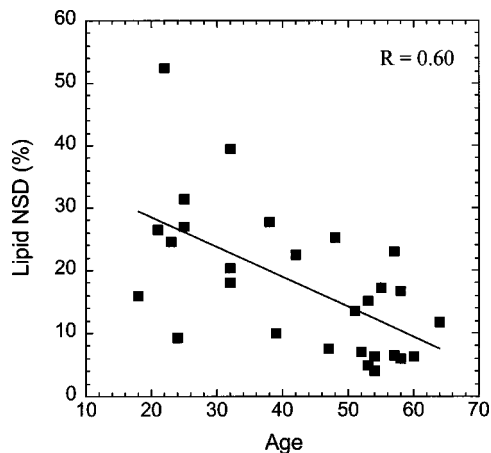


**Fig. 7** The normalized standard deviation (NSD) to the mean lipid concentration for the eight quadrant sites versus age for the 28 volunteers. The line represents a linear least-squares fit to the data.

scattering on average than outer quadrants (approximately  $0.05$  to  $0.1 \text{ mm}^{-1}$ ) for both subject groups (77 and 92% confidence intervals for right and left breasts, respectively).

The wavelength dependence of scattering (i.e., scatter power) is influenced by the fat, collagen, and epithelial content. The scatter power ( $\mu_s' = A\lambda^{-\text{scatter power}}$ ) is shown for each position in Fig. 6(b). PRE women have a scatter power that is 1.5-fold higher than POST women. The areolar scatter power is 30 to 60% greater in PRE women, and 15 to 30% greater in POST women (99 and 88% confidence intervals for left and right breasts, respectively). The right areola has a larger scatter power than the left on average by about 15 to 25% (97% confidence interval).

The normalized standard deviation of the physiological parameters over the eight breast quadrants was calculated for each of the volunteers to quantify the variability typically found in healthy breast, and to investigate age-related changes in heterogeneity. Only lipid content showed significant changes in heterogeneity with age (Fig. 7). PRE and POST women typically ( $\geq 89\%$  of volunteers) have a NSD of 30% or lower for adipose tissue, and lipid heterogeneity decreases with age ( $R=0.60$ ). The NSD is typically ( $\geq 89\%$  of volunteers) less than 40% for THC, less than 30% for water, less than 12% for  $\mu_s'$  (at 674 nm), and less than 25% for the scatter power. The normalized standard deviation for  $S_tO_2$  is less than 12% for all but one (97%) of the 28 individuals.

**Table 2** Mean deviation between left and right breasts for 28 individuals (%).

	Water	THC	Scatter power	Lipid	$\mu_s'$
Upper outer quadrant	13	31	22	20	7
Other quadrants	11	25	10	15	7
Areolar	25	18	26	40	9

A small degree of asymmetry between breasts is common in women. To examine the differences between the right and left breasts of healthy individuals, the relative difference ( $(\text{right-left}/\text{average}) * 100\%$  for the four quadrants of each subject was measured (Table 2). Although differences between right and left breasts exist in individuals, the results found no consistent differences between the right and left breasts in the population for  $\mu_s'$ , water, lipid, THC, or  $S_tO_2$ . The right areolar region, however, has significantly higher mean scatter power values than the left, and equal or greater values were measured in 23/26 cases. The question of whether there is regular breast volume asymmetry remains unsolved.<sup>27–29</sup> The relative difference between symmetric positions can range from 18 to 30% for THC, 10 to 40% for adipose, 10 to 25% for water, and 4 to 9% for scattering (674 nm), depending on position (Table 2).

## 4 Discussion

Optical techniques for breast cancer detection are based on the assumption that differences in tissue absorption and scattering can provide a basis for tumor characterization and clinical management. Thus, the accuracy and efficacy of optical mammography requires detailed study of the multiple factors affecting breast tissue heterogeneity and composition. Breast tissue is nonuniform; furthermore, physiological changes that occur over a woman's lifetime can affect the distribution and composition of healthy breast tissue. With the onset of menopause, glandular tissue involutes and is replaced by adipose, which produces a new spatial distribution of chromophores. In addition, this process is nonuniform, which changes the inherent heterogeneity of the breast tissue.<sup>30</sup> Reduced scattering ( $\mu_s'$  and tissue hemoglobin oxygen saturation ( $S_tO_2$ )) showed  $\leq 12\%$  variation over the entire breast and  $\leq 6\%$  over a 3-cm region. Alterations in  $\mu_s'$  or  $S_tO_2$  may signify regions of breast disease. Previous studies have shown that increased spatial heterogeneity in scattering may be indicative of normal tissue or benign breast disease, while regions of more uniform scattering may suggest invasive cancer.<sup>11</sup> Significantly higher  $\mu_s'$  values observed for the inner quadrants [Fig. 6(a)] may be due to contributions of the sternal border and pectoralis muscle to the optical signal. Changes in total hemoglobin over small regions of tissue (5 to 11%) may be attributed to spatial variations in underlying blood vessels in the probed tissue volume.

In PRE women, the areolar region displayed 25 to 30% lower lipid content, 30 to 50% higher water content, 30 to 60% higher scatter power, and 5% lower  $S_tO_2$  values when compared to the quadrants (Figs. 3–6). These results are consistent with the unique physiology of the areola. Since lactiferous ducts open at the surface of the nipple, glandular tissue is concentrated and superficial at the areola.<sup>31</sup> The ducts are surrounded by highly vascularized connective tissue; therefore, our measurements of elevated hemoglobin and reduced adipose content in this region of the breast are consistent with known breast structure.<sup>31</sup> Lower  $S_tO_2$  at the areola may be due to the higher metabolic demands of glandular tissue.<sup>31,32</sup> The areolar complex lacks fat and is mostly comprised of dense fibrous tissue and smooth muscle; the surrounding pigmented areola contains apocrine and eccrine glands.<sup>33</sup> As a result, the areola has a greater scatter power, indicative of

smaller scattering particles. In POST women, the areolar region had 25 to 40% higher hemoglobin, 10% lower lipid content, and 15 to 30% greater scatter power. Since glandular tissue is replaced with fat after menopause, the optical contrast of the areolar region is less pronounced in POST subjects.<sup>31</sup> Deeper pigmentation of the areolar region may play a role in the increased absorption and scattering values. However, the contrast of the areola is less pronounced in POST women, which suggests that the differences in optical parameters at this location are mainly physiological and anatomical.

Spatial heterogeneity in lipid and water content can be attributed to the nonuniform distribution of glandular structures in the breast. Glandular tissue contains higher water content than adipose tissue due to the higher water content of ductal epithelial cells and connective tissue compartments. Thus regions of higher lipid or higher water content arise, depending on whether the volume of tissue sampled is mostly fatty or glandular.

Intrasubject lipid spatial heterogeneity decreases as a function of age (Fig. 7). These results are consistent with glandular tissue composition and atrophy that accompanies menopause. The premenopausal breast consists of glandular structures embedded in fat. As a result, the spatial heterogeneity of adipose tissue in younger women is greater than in older women who have a more uniform distribution of adipose. Figure 7 shows that the spread of NSD values is larger for younger women and decreases with age. The volume of glandular tissue and fat vary with breast size.<sup>33</sup> Thus in a population of premenopausal women of varying breast size, there is a wide range of NSD values.

The NSD values calculated for water and total hemoglobin concentration show that the variability for these parameters over both breasts is typically less than 30 or 40%, respectively, which reflects the intrinsic heterogeneity of healthy breast anatomy. Since previous studies show that tumor tissue can exhibit 2- to 4-fold higher THC and water levels than surrounding breast tissue,<sup>9–11</sup> optical techniques have promise for characterizing and detecting certain lesions. However, sensitivity is highly dependent on the lesion size and type, and whether exogenous contrast-enhancing agents are employed.<sup>34,35</sup> Furthermore, contrast based on measurements of the symmetric location on the uninvolved breast can be problematic.<sup>36</sup> This is due to our observation of large differences between the left and right breasts in most physiological parameters. Interestingly, this feature may have diagnostic utility, since recent studies suggest that substantial breast asymmetry may be indicative of breast cancer risk.<sup>37</sup>

## 5 Summary

The intra- and inter-subject spatial variations of the optical and physiological parameters of 31 subjects are investigated using diffuse optical spectroscopy. Small-scale variations (3 cm) are found to be negligible compared to larger variations over the whole breast. Our results show that the properties of the areolar complex are unique compared to the four main quadrants, and glandular tissue distribution plays an important role in baseline optical properties of the breast. These differences are clearly age- and hormone-dependent. In addition, bilateral asymmetry can be significant in an individual, al-

though no consistent right-left differences are observed in a population. The intrinsic spatial heterogeneity of healthy breast tissue is 20 to 40% for  $\mu_a$  and 5 to 12% for  $\mu_s'$ . These values are important because they establish the fundamental sensitivity limits for detecting breast disease based on optical contrast.

## Acknowledgments

This work was made possible by a National Institutes of Health funded facility, the Laser Microbeam and Medical Program (#RR-01192), the California Breast Cancer Research Program (#P20-CA86182), and the Avon Foundation-Chao Family Comprehensive Cancer Center. Author Cerussi acknowledges support from the U.S. Army Medical Research and Material Command (DAMD17-98-1-8186). Beckman Laser Institute programmatic support is provided by the Air Force Office of Scientific Research (AFOSR) and the Beckman Foundation. Finally, the authors wish to thank the patients who generously volunteered for the study.

## References

1. S. Merritt, F. Bevilacqua, A.J. Durkin, D.J. Cuccia, R. Lanning, B.J. Tromberg, G. Gulsen, H. Yu, J. Wang, and O. Nalcioglu, "Coregistration of diffuse optical spectroscopy and magnetic resonance imaging in a rat tumor model," *Appl. Opt.* **42**, 2951–2959 (2003).
2. D.J. Cuccia, F. Bevilacqua, A.J. Durkin, S. Merritt, B.J. Tromberg, G. Gulsen, H. Yu, J. Wang, and O. Nalcioglu, "In vivo quantification of optical contrast agent dynamics in rat tumors by use of diffuse optical spectroscopy with magnetic resonance imaging coregistration," *Appl. Opt.* **42**, 2940–2950 (2003).
3. V. Ntzichristos, A.G. Yodh, M.D. Schnall, and B. Chance, "MRI-guided diffuse optical spectroscopy of malignant and benign breast lesions," *Neoplasia* **4**(4), 347–354 (2002).
4. Q. Zhu, N. Chen, and S.H. Kurtzman, "Imaging tumor angiogenesis by use of combined near-infrared diffusive light and ultrasound," *Opt. Lett.* **28**, 337–339 (2003).
5. M.J. Holboke, B.J. Tromberg, X. Li, N. Shah, J. Fishkin, D. Kidney, J. Butler, B. Chance, and A.G. Yodh, "Three-dimensional diffuse optical mammography with ultrasound localization in a human subject," *J. Biomed. Opt.* **5**(2), 237–247 (2000).
6. D.B. Jakubowski, A.E. Cerussi, F. Bevilacqua, N. Shah, D. Hsiang, J. Butler, and B.J. Tromberg, "Monitoring neoadjuvant chemotherapy in breast cancer using quantitative diffuse optical spectroscopy: a case study," *J. Biomed. Opt.* **9**(1), 230–238 (2004).
7. N. Shah, A.E. Cerussi, C. Eker, J. Espinoza, J. Butler, J. Fishkin, R. Hornung, and B.J. Tromberg, "Noninvasive functional optical spectroscopy of human breast tissue," *Proc. Natl. Acad. Sci. U.S.A.* **98**, 4420–4425 (2001).
8. A.E. Cerussi, A.J. Berger, F. Bevilacqua, N. Shah, D. Jakubowski, J. Butler, R.F. Holcombe, and B.J. Tromberg, "Sources of absorption and scattering contrast for near-infrared optical mammography," *Acad. Radiol.* **8**, 211–218 (2001).
9. S. Fantini, S.A. Walker, M.A. Franceschini, M. Kaschke, P.M. Schlag, and K.T. Moesta, "Assessment of the size, position, and optical properties of breast tumors *in vivo* by noninvasive optical methods," *Appl. Opt.* **37**, 1982–1989 (1998).
10. B.W. Pogue, S.P. Poplack, T.O. McBride, W.A. Wells, K.S. Osterman, U.L. Osterberg, and K.D. Paulsen, "Quantitative hemoglobin tomography with diffuse near-infrared spectroscopy: pilot results in the breast," *Radiology* **218**, 261–266 (2000).
11. B.J. Tromberg, N. Shah, R. Lanning, A. Cerussi, J. Espinoza, T. Pham, L. Svaasand, and J. Butler, "Non-invasive *in vivo* characterization of breast tumors using photon migration spectroscopy," *Neoplasia* **2**, 1–15 (2000).
12. J.B. Fishkin and E. Gratton, "Propagation of photon-density waves in strongly scattering media containing an absorbing semi-infinite plane bounded by a straight edge," *J. Opt. Soc. Am. A* **10**, 127–140 (1992).
13. M. Cope, "The application of near-infrared spectroscopy to non-invasive monitoring of cerebral oxygenation in the newborn infant,"

- University College London, Dept. Medical Phys. *Bioeng.*, London, England (1990).
14. E.M. Sevick, B. Chance, J. Leigh, and S. Nioka, "Quantitation of time-resolved and frequency-resolved optical spectra for the determination of tissue oxygenation," *Anal. Biochem.* **195**, 330–351 (1991).
  15. B. Beauvoit, T. Kitai, and B. Chance, "Contribution of the mitochondrial compartment to the optical properties of the rat liver—a theoretical and practical approach," *Biophys. J.* **67**, 2501–2510 (1994).
  16. A.M.K. Nilsson, C. Stureson, D.L. Liu, and S. Andersson-Engels, "Changes in spectral shape of tissue optical properties in conjunction with laser-induced thermotherapy," *Appl. Opt.* **37**, 1256–1267 (1998).
  17. V. Ntziachristos, A.G. Yodh, M. Schnall, and B. Chance, "Concurrent MRI and diffuse optical tomography of breast after indocyanine green enhancement," *Proc. Natl. Acad. Sci. U.S.A.* **97**, 2767–2772 (2000).
  18. R. Cubeddu, C. D'Andrea, A. Pifferi, P. Taroni, A. Torricelli, and G. Valentini, "Effects of the menstrual cycle on the red and near-infrared optical properties of the human breast," *Photochem. Photobiol.* **72**, 383–391 (2000).
  19. T.H. Pham, O. Coquoz, J.B. Fishkin, E. Anderson, and B.J. Tromberg, "Broad bandwidth frequency domain instrument for quantitative tissue optical spectroscopy," *Rev. Sci. Instrum.* **71**, 2500–2513 (2000).
  20. J. Fishkin, E. Gratton, M.J. Vandeven, and W.W. Mantulin, "Diffusion of intensity modulated near-infrared light in turbid media," *Proc. SPIE* **1431**, 122–135 (1991).
  21. J.B. Fishkin, S. Fantini, M.J. Vandeven, and E. Gratton, "Gigahertz photon density waves in a turbid medium—theory and experiments," *Phys. Rev. E* **53**, 2307–2319 (1996).
  22. J.B. Fishkin and E. Gratton, "Propagation of photon-density waves in strongly scattering media containing an absorbing semi-infinite plane bounded by a straight edge," *J. Opt. Soc. Am. A* **10**, 127–140 (1993).
  23. R.C. Haskell, L.O. Svaasand, T.T. Tsay, T.C. Feng, M.S. McAdams, and B.J. Tromberg, "Boundary conditions for the diffusion equation in radiative transfer," *J. Opt. Soc. Am. A* **11**, 2727–2741 (1994).
  24. G.M. Hale and M.R. Querry, "Optical constants of water in the 200 nm to 200  $\mu\text{m}$  wavelength region," *Appl. Opt.* **12**, 555–563 (1973).
  25. S. Wray, M. Cope, D.T. Delpy, J.S. Wyatt, and E.O. Reynolds, "Characterization of the near-infrared absorption spectra of cytochrome aa3 and haemoglobin for the non-invasive monitoring of cerebral oxygenation," *Biochim. Biophys. Acta* **933**, 184–192 (1988).
  26. C. Eker, "Optical characterization of tissue for medical diagnostics," Lund University Medical Laser Centre, Dept. of Physics, Lund Institute of Technology, Lunden, Sweden (1999).
  27. D.J. Smith, Jr., W.E. Plain, Jr., V.L. Katch, and J.E. Bennett, "Breast volume and anthropomorphic measurements: normal values," *Plast. Reconstr. Surg.* **78**, 331–335 (1986).
  28. Q. Qiao, G. Zhou, and Y. Ling, "Breast volume measurements in young Chinese women and clinical applications," *Aesthetic Plast. Surg.* **21**, 362–368 (1997).
  29. T.P. Brown, C. Ringrose, R.E. Hyland, A.A. Cole, and T.M. Brotherson, "A method of assessing female breast morphometry and its clinical application," *Br. J. Plast. Surg.* **52**, 355–359 (1999).
  30. B.G. Wren, "The breast and the menopause," *Baillieres Clin. Obstet. Gynaecol.* **10**, 433–447 (1996).
  31. S.A. Bartow, *Pathology*, 2nd ed., E. Rubin and J.L. Farber, Eds., pp. 973–977, J.B. Lippincott, Philadelphia, PA (1994).
  32. J.E. Berkowitz, O.M. Gatewood, L.E. Goldblum, and B.W. Gayler, "Hormonal replacement therapy—mammographic manifestations," *Radiology* **174**, 199–201 (1990).
  33. K.J. Berger, *A Woman's Decision: Breast Care, Treatment and Reconstruction*, 3rd ed., K.J. Berger and J. Bostwick, Eds., "Breast anatomy and physiology," pp. 7–12, Quality Medical Publishing, St. Louis, MO (1998).
  34. X. Intes, J. Ripoll, Y. Chen, S. Nioka, A.G. Yodh, and B. Chance, "In vivo continuous-wave optical breast imaging enhanced with indocyanine green," *Med. Phys.* **30**, 1039–1047 (2003).
  35. G. Gulsen, H. Yu, J. Wang, O. Nalcioglu, S. Merritt, F. Bevilacqua, A.J. Durkin, D.J. Cuccia, R. Lanning, and B.J. Tromberg, "Congruent MRI and near-infrared spectroscopy for functional and structural imaging of tumors," *Technol. Cancer. Res. Treat.* **1**, 497–505 (2002).
  36. B.J. Tromberg, O. Coquoz, J.B. Fishkin, T. Pham, E.R. Anderson, J. Butler, M. Cahn, J.D. Gross, V. Venugopalan, and D. Pham, "Non-invasive measurements of breast tissue optical properties using frequency-domain photon migration," *Philos. Trans. R. Soc. London. Ser. B-Biol. Sci.* **352**, 661–668 (1997).
  37. D. Scutt, J.T. Manning, G.H. Whitehouse, S.J. Leinster, and C.P. Massey, "The relationship between breast asymmetry, breast size and the occurrence of breast cancer," *Br. J. Radiol.* **70**, 1017–1021 (1997).